

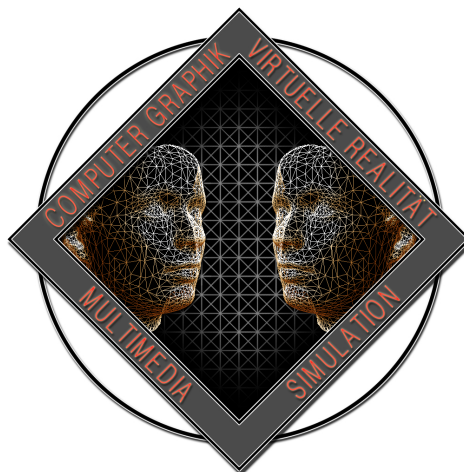
## BACHELOR'S THESIS

---

# Computation of BCSDFs for elliptical multi-fiber bundles

---

Marvin Wallenfang



INSTITUTE OF COMPUTER SCIENCE II – VISUAL COMPUTING  
UNIVERSITY OF BONN

First Reviewer: Prof. Dr. Rheinhard Klein  
Second Reviewer: Prof. Dr. Matthias Hullin

February 16, 2024



# Summary

---

Often fibers do not occur in isolation, but rather as part of a bundle of fibers. Investigating how the scattering of light changes for different arrangements of fibers can be important to figure out how the rendering of such structures can be done more efficiently.

In this thesis, a framework was developed to investigate how the light scattering changes for different arrangements of fibers in a structure. The framework traces rays through the structure and records the outgoing radiance in a tabulated form. For circular arrangements, the result is a uniformly blurred version of the input data, while this blurring effect is dependent on the respective radii for elliptical arrangements.

This shows that the density and the structure do influence how the resulting model differs from the input model.



# Acknowledgments

---

I want to thank my advisor M.Sc. Tom Kneiphof for his support and guidance throughout the entire work. Especially for the help with implementing it using Mitsuba, as well as several derivations as well as ideas for the whole process.

I would also like to thank my family and friends for their continuous support throughout my studies up until now, as well as this thesis.



# Contents

---

<b>1</b>	<b>Introduction</b>	<b>1</b>
1.1	Related Works . . . . .	2
<b>2</b>	<b>Background</b>	<b>5</b>
2.1	Structure of yarn . . . . .	5
2.2	Fiber shading model . . . . .	6
2.3	Wave effects . . . . .	7
<b>3</b>	<b>Method</b>	<b>9</b>
3.1	Single fiber model . . . . .	9
3.2	Integrating over the bundle . . . . .	10
3.3	Integration into Mitsuba 3 . . . . .	12
<b>4</b>	<b>Validation</b>	<b>15</b>
4.1	Single fiber . . . . .	15
4.2	Two fibers . . . . .	16
<b>5</b>	<b>Results</b>	<b>19</b>
5.1	Circular arrangement . . . . .	20
5.2	Elliptical Arrangement . . . . .	21
5.3	Rendered . . . . .	22
<b>6</b>	<b>Summary</b>	<b>25</b>
6.1	Future work . . . . .	25
<b>Bibliography</b>		<b>29</b>

## CONTENTS

---

# 1

## Introduction

---

Structures made of fibers exist everywhere in day-to-day life and thus they are also very prominent in rendering realistic scenes. Be it clothing, knitwear, hair or even furniture, all of these consist of fibers, where the big differences are their size and the structure of how they are combined, besides which fibers are used to begin with. Due to the common occurrence of materials made of fiber, it is important to examine the light interaction with such materials to allow for realistic renderings, since they are part of many scenes.

There is also a difference in how materials made with singular fibers like hair or fur are rendered, compared to materials made of yarn or cloth, where the fibers are wound together resulting in a different light interaction. Here for a very realistic result, each fiber has to be taken into account, which quickly becomes very expensive to compute. The difficulty of rendering such materials stems from the high density of fibers in the material and so a very high amount of bounces happen in a very small space. So approximations have to be made to allow for more efficient computation.

A typical piece of thread consists of several tightly wound plies that contain several hundreds of fibers each. The fibers inside of the plies are called regular fibers, to discern them from the flyaway fibers. The flyaway fibers are stray fibers that are randomly placed and oriented. They appear due to inaccuracies during winding, as well as natural wear and tear of the material.

One of the common approximations that is employed in rendering, is to ignore the wave optics effects that occur during the light interaction with the fibers. This happens due to the thin nature of the fibers, causing the light to be diffracted. Xia, Walter, Michielssen, et al. (2020) have shown that this causes a lot of colorful glints for single fibers, which softens the overall appearance.

This thesis focuses on the impact that these effects have on the appearance of bundles of fibers, like yarn or several wound-together single fibers. The specific scenario that is examined is in the case of spectral rendering, where in addition to the surface directions, the wavelength also changes the model. The main example for the modeling of the method, as well as the rendering of the results, will be a ply of a piece of yarn since that is a common structure in knitwear. It is also intuitive to reason about the functionality of the developed framework at the example of a single

## 1.1. RELATED WORKS

---

ply. But any bundle that can be rendered as a curve can be used as a structure for the framework.

To gather the light interaction data for the structures, a rendering framework was developed that allows for the computation of any custom bundle of parallel fibers. For this, the framework uses an input fiber model that differs depending on the wavelength of light and uses common ray-based rendering to estimate the light interaction for this specific wavelength. This is then run for the whole visible light spectrum and aggregated into a resulting model that can be inspected and used for rendering.

Many approaches estimate the light interaction for the whole yarn or use a simplified model for the light interaction with the fibers. Although there are some methods that view the yarn as a volume and estimate the density of the yarn (Xu et al., 2001).

## 1.1 Related Works

The field of rendering knitwear and cloth can be split up into three categories of geometric representations. The typical method of representing the geometry of a piece of cloth is to view it as a surface upon which single fibers are not being considered, but rather the surface is modeled as a surface. Another approach is to view the geometry as a volume, where the density of the material at different points is estimated. An advantage of this method is that it can display details in close-up views, which would be lost in a surface representation. The third approach that this thesis is also focused on is the representation of curves. In this, each yarn, ply or fiber is represented as a curve, to which the light interaction is applied.

The different works related to curve rendering can be split up into two categories. The ones who use ray-based methods, where the light is represented as a ray carrying radiance, which is the most common method for general rendering. And the ones who use wave-based methods, where the light is represented as samples over the wavelength spectrum so that the light behaviors at different colors can be properly represented. These have primarily been developed in recent years to investigate the impact of diffraction on the light interaction with fibers.

### 1.1.1 Ray-based fiber and yarn models

S. R. Marschner et al. (2003) first introduced an approach that is very widespread today where the interaction with the fiber is modeled using two functions, one for the longitudinal portion and one for the azimuthal portion. These functions are further split up into three lobes each. Each lobe describes a different path that a ray might take inside of the fiber.

d'Eon et al. (2011) improved the model by developing an energy-conserving model, which is more robust for fibers that absorb less light. These weren't properly represented in the model by S. R. Marschner et al. (2003) due to simplifications that were made during it.

## CHAPTER 1. INTRODUCTION

---

These two models are built to create very realistic results, which might be a hindrance for more artistic applications where an artist might want more control over the look of the fibers. For this purpose Sadeghi et al. (2013) developed a model where the artist can control the intensity, color and position of the highlights in the fibers.

Irawan and S. Marschner (2012) used a combination of a textural approach as well as a curve-based yarn approach to calculate the specular highlights of cloth

The procedural modeling of irregularities in yarn and cloth, like flyaway fibers, was explored by Zhao et al. (2016). They developed methods for fitting procedural models to measured yarns, as well as methods of constructing the irregularities.

The differences in the shapes of different fibers were investigated by Aliaga et al. (2017). There it was shown that the type of fiber and its microgeometry have a lot of influence on the resulting appearance of the cloth.

### 1.1.2 Wave-based fiber and yarn models

Xia, Walter, Michielssen, et al. (2020) simulated the wave optics effects of light interacting with a single fiber using the boundary element method. This resulted in a very accurate model, but it is also very computationally expensive during the simulation as well as the rendering. They found that the wave effects are especially visible in the highlights of the fiber since the differing wavelengths cause the highlights to be softened and to create more colorful glints.

Due to that Xia, Walter, Hery, et al. (2023) further developed this model to be more efficient during the simulation, as well as including the effects of micro geometry of the fibers in the resulting models. They also fitted the resulting data to a set of noise functions that approximate the model, to further improve the performance of the method. This is also the model that was used as an input to this thesis to build upon when creating a model for yarn.

## 1.1. RELATED WORKS

---

# 2

# Background

---

This chapter gives a more in-depth introduction to the structure of yarn, the general basics for fiber shading models, especially their differences to the common BSDF models, as well as the wave effects that can occur during the light interaction with thin fibers.

## 2.1 Structure of yarn

A piece of yarn consists of several plies that are tightly wound around one another or an additional center ply. The amount of plies, as well as the rate of the winding, can differ between different yarns. Each ply can be described as a circular bundle of fibers. On top of that, there are also flyaway fibers, which are irregular fibers that poke out of the yarn and are randomly spread out. (Zhao et al., 2016)

The structure of a ply is very fitting for the framework that was developed for this thesis since it consists of tightly packed fibers, arranged in a mostly circular shape. Due to the tightly packed structure, the output directions of the rays will be somewhat uniformly spread out along the whole circle. In the case of less tightly packed structures, there might be regions where only a few rays end up, which slows down the convergence in those regions.

Thus it is interesting to also investigate how a piece of yarn can be structured using the plies.

Zhao et al. (2016) have derived functions to describe the winding of the plies around the z-axis:

$$\begin{aligned} S_x(z) &= R^{ply} \cos\left(\frac{2\pi z}{\alpha^{ply} + \Theta^{ply}}\right) \\ S_y(z) &= R^{ply} \sin\left(\frac{2\pi z}{\alpha^{ply} + \Theta^{ply}}\right) \end{aligned} \tag{2.1}$$

Where  $R^{ply}$  describes the radius of the ply,  $\alpha^{ply}$  describes the pitch of the ply and  $\Theta^{ply}$  the angle.

## 2.2 Fiber shading model

The BCSDF (Bidirectional Curve Scattering Distribution Function) describes the scattering on a curve structure, with the incoming and the outgoing angles. In the case of spectral rendering, the wavelength is an additional parameter. (Xia, Walter, Michielssen, et al., 2020)

This results in the very similar integration formula to the common BSDF, although in this case, the integration happens over the full surrounding sphere since the light can come from any direction:

$$L_o(\omega_o, \lambda) = \int L_i(\omega_i) S(\omega_i, \omega_o, \lambda) \cos(\theta_i) d\omega_i \quad (2.2)$$

The angles are defined as polar coordinates, so the function that will be calculated in the thesis will be the following with five dimensions:

$$S(\varphi_i, \theta_i, \varphi_o, \theta_o, \lambda) \quad (2.3)$$

Due to the spectral integration, the integration formula at the sensors also differs from the commonly used path integration function:

$$\begin{aligned} I_r &= \int_0^\infty c_R(\lambda) \cdot L(\lambda) d\lambda \\ I_g &= \int_0^\infty c_G(\lambda) \cdot L(\lambda) d\lambda \\ I_{br} &= \int_0^\infty c_B(\lambda) \cdot L(\lambda) d\lambda \end{aligned}$$

Here  $I_x$  represents the integration for the three color-channels, with  $c_x$  being the color-matching function for the respective channel.

The structure of the polar coordinates is a bit different than the normal one, as the  $\theta$  angles are relative to the orthogonal plane of the fiber, rather than the z-axis. This is visualized in figure 2.1.

The practical reasoning for this coordinate system is that by defining the  $\theta$  angles to be relative to the x-y plane, the y-axis can be set to be the tangent of the fiber. Thus the angles can be normalized to be relative to the fiber section using the orthogonal to its tangent, since the  $\theta$  angle will be relative to this orthogonal.

Another consideration that is important for knitwear is that due to the thickness of the plies a

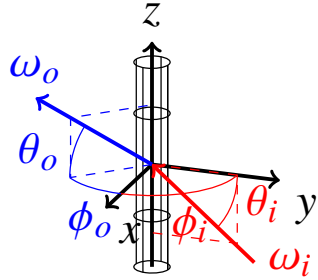


Figure 2.1: The polar coordinate system used for the incoming and outgoing directions in the fibers.

BSSRDF model is required since the light enters the ply at a different point than it leaves it. For that, the outgoing position has to be found on the models, which is further discussed in section 3.2.

## 2.3 Wave effects

Effects on the light interaction with fibers can differ between different wavelengths due to the effects of diffraction inside and around fibers since their width is normally in a similar order of magnitude as visible light.

As an example, human hair fibers tend to be around  $50\text{-}100\mu\text{m}$  in width. (Zhao et al. (2016)) Since visible light is around  $0.4\text{-}0.7\mu\text{m}$  in wavelength, diffraction patterns can occur inside and around human fibers.

Xia, Walter, Michielssen, et al. (2020) have shown that the effect of diffraction has a big impact on the appearance of single fibers. The biggest impact comes from colorful highlights in the fibers because different wavelengths are diffracted differently, which causes them to be spread out in slightly different directions. This also causes every structure to appear softer, compared to ray-based models.

### 2.3. WAVE EFFECTS

---

# 3

# Method

---

In this chapter, the way towards achieving the goal of building a general framework for creating the output model based on an input model is explained. In total, it consists of three steps, where the first and third step depends on the model that is used as an input, as well as the renderer that is used in the end.

## 1. Gathering the model for a singular fiber

For this implementation the model by Xia, Walter, Hery, et al. (2023) is used, which models the light transport through a single fiber with microgeometry based on differing wavelengths.

## 2. Bundling the singular models into a bundle BCSDF

The bundled BCSDF is created by simulating the light transport through the fiber bundle geometry by shooting rays through it. The data is then tabulated into a numpy array.

## 3. Sampling the tabulated bundled BCSDF

The tabulated data is then sampled inside of a Mitsuba 3 BSDF. An integrator to facilitate differing input and output positions is also implemented.

### 3.1 Single fiber model

In this implementation the single fiber model by Xia, Walter, Hery, et al. (2023) is used. Any model that allows for the wavelength interaction of light can be used. This model was chosen due to the optimization of its simulation, which makes it possible to use in the scope of this thesis.

The model uses a 3d representation of the fiber with its microgeometry on the surface as its basis and splits it up into many small segments. These segments are used as a basis for an oc-tree, using which the influence of the light waves on each level is aggregated.

The surface of that oc-tree is then used to approximate the far-field light response of the fiber segment.

### 3.2. INTEGRATING OVER THE BUNDLE

---

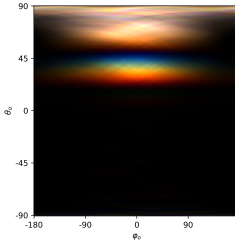


Figure 3.1: An example of the model for  $\theta_i = 165^\circ$ . Each wavelength is scattered at different angles resulting in the colorful highlights.

The resulting tabulated data is the far-field light scattering of the fiber with a specific incident direction.

An example can be seen in 3.1. An important note in the implementation is that the chosen model is for a circular fiber. Thus the difference in the longitudinal ( $\varphi_i$ ) rotation of the input model is not taken into account, since it does not change the resulting scattering. This is done to simplify the implementation a bit and to reduce the dimensions of the data to be stored on the GPU.

For elliptical fibers the longitudinal rotation has to be taken into account as well, which adds a dimension to the input data.

In the following chapters, the model for fiber\_0 by Xia, Walter, Hery, et al. (2023) is used, which is a circular fiber with uniformly spaced surface speckles and without cuticles. This structure closely resembles the structure of polyester fibers.

The specific features of this model are examined in more depth in 5.

## 3.2 Integrating over the bundle

Each sample of the wavelengths is run separately. This saves a dimension in the data additionally to the  $\varphi_i$  dimension to result in a 3d table for the input data, which can be efficiently sampled on the GPU.

The bundle of fibers that should be integrated is made up of vertical cylinders with a set radius and position. These can be arbitrarily positioned, although structures with big gaps or non-elliptical shapes might not be perfectly suited to be rendered on elliptical curved surfaces in the end. As an example, the model for a single ply of yarn is being utilized which can be created using Poisson Disk Sampling, where the minimum distance between elements corresponds with double the radius. Then after creating the model each element that is outside of a circle with the bundle radius is discarded to end up with a randomized spread of fibers in a circle. The method of discarding elements can be used to generate any shape by simply discarding the elements outside of its bounds.

## CHAPTER 3. METHOD

---

From the resulting structure, a bounding circle is created, which is used to set the starting positions for the incident rays later on. This is defined by setting its middle point to half of the width in each direction and setting its radius to the maximum distance from that point.

On this circle, the starting positions are set according to the starting direction. From that point and direction, a randomized position along the side vector of that direction is set to randomize the incident locations into the structure while maintaining the direction. This is done to capture all the details for the incident rays instead of just the middle.

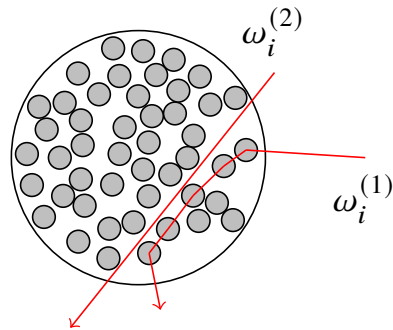


Figure 3.2: Two possible paths through the fiber bundle for rays. For readability the ray directions were changed to hit the center of each fiber. A correct path would hit the surface and then continue from a random position on the surface in the continuation direction. There are cases where a ray might not hit a fiber at all. Those are dealt with separately.

With each intersection of a ray and a cylinder, a random outgoing direction is sampled by uniformly sampling  $\varphi_o$  and  $\theta_o$  separately. This is done rather than sampling it uniformly on a sphere because the output model will also be equally spaced on  $\varphi_o$  and  $\theta_o$ . Sampling the outgoing direction uniformly on a sphere would introduce artifacts at the boundaries of  $\theta_o$  due to the non-linear density of samples along  $\theta_o$ .

Using this direction the surface of the cylinder is calculated. For the outgoing direction, the ray is shifted along the side direction from the outgoing direction. This way the different paths the ray can take are simulated statistically. The shift does not occur in the z-direction, since the fibers are all parallel and that would not result in any changes in the path of the ray aside from a z-offset. An example of the shift is shown in figure 3.3.

The point on the surface can be calculated for circular cylinders as follows:

$$p_{\text{out}} = p_{\text{cyl}} + \left( \frac{r}{\sqrt{1 - \langle \omega_{\text{out}}, \omega_{\text{in}} \rangle^2}} \right) * \omega_{\text{out}}$$

$$p_{\text{out\_shifted}} = p_{\text{out}} + \text{shift} \cdot (\omega_{\text{fiber}} \times \omega_{\text{out}})$$

### 3.3. INTEGRATION INTO MITSUBA 3

---

Where  $p_{cyl}$  is the point in the middle of the cylinder,  $\omega_{out}$   $\omega_{in}$  are the outgoing and incident direction and  $r$  is the radius of the cylinder. Afterwards, this position is shifted along the side vector of the direction of the fiber and the outwards direction to send them out along the plane perpendicular to the direction of the fiber.

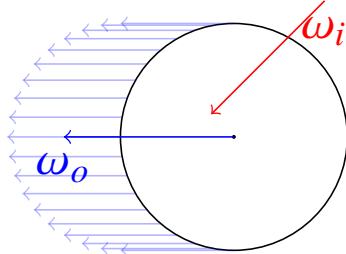


Figure 3.3: The outgoing direction is shifted along its side vector to simulate the different transmission paths it might take inside of the fiber. The outgoing middle of the shift is always the middle of the fiber. Thus it is invariant to the incoming direction. Just the intensity of the outgoing ray depends on the incoming and outgoing directions.

The intensity of the outgoing ray is then multiplied by the value in the tabulated BCSDF for the pair of incident and outgoing directions.

This is repeated until either the bounce limit is reached or a ray leaves the bundle. The latter case is handled by checking if there are any valid intersections for a ray. If there are none, then the ray is assumed to have left the bundle and the ray is terminated. If the maximum bounce depth is reached then the ray is terminated, but set to be invalid, so that no contribution is added to the resulting table.

The resulting rays are then aggregated into a numpy table. All the rays that did not hit anything are not added to that table, but rather they're saved separately as a ratio to know what amount of light passes straight through the bundle without hitting anything. This ratio is used in 3.3 to decide if a ray should interact with a bundle or not.

All the resulting tables for the different directions are then aggregated into a 5d table that is saved into a file for further usage.

## 3.3 Integration into Mitsuba 3

For the rendering of the results, the Mitsuba 3 library by Jakob et al. (2022) is used. Mitsuba 3 already implements a lot of optimizations, as well as support for different hardware, which is why it is being used.

Two new elements had to be implemented to render the results. A new BSDF, which supports the tabulated input, as well as an integrator that can use the differing input and output positions, together with the BSDF.

---

## CHAPTER 3. METHOD

---

First, the BSDF evaluates the passthrough chance of the current ray and sets the return value accordingly to tell the integrator whether or not to pass through the element. If the ray does interact with the element, then the BSDF uniformly samples the direction in which it will be sent out of the element. From the new direction, as well as the incident direction the phi and theta angles are calculated relative to the surface of the curve.

One downside of Mitsuba, in this case, is that it only supports textures up to 3 dimensions, so the 5-dimensional scattering data has to be read into a Mitsuba Tensor to then be addressed linearly. The addressing of the linear array is done as follows:

$$\text{linear\_index} = \sum_{i=0}^4 \prod_{k=i}^4 (\text{shape}_k) \cdot \text{index}_i$$

Where  $\text{size}_k$  is the size of the k-th dimension and  $\text{index}_i$  is the index in the i-th dimension.

The resulting value is then returned as the BSDF value after applying the Lambertian Cosine Law.

For the integrator, the resulting BSDF data is used, where first it is checked whether the ray should interact with the object or if it should simply pass through. If the ray should pass through the object, then the integrator calls the `get_out_position` function of the respective shape, which returns a position on the shape's surface for an outgoing direction. Here the integrator passes the same direction as the incident direction. The position that is returned is then set for a new way which continues in the same direction, but with the updated position on the other side of the object.

If the ray should interact with the object, then the integrator also calls the `get_out_position` function of the interacted shape but sets the outgoing direction to be the one that was returned by the BSDF. It also sets the shift along the side vector of the outgoing direction and the direction of the fiber to be a random value, so that there is no bias towards the center of the curve.

### 3.3. INTEGRATION INTO MITSUBA 3

---

# 4

# Validation

---

In this chapter, the results of the framework are validated against the input model. It is also investigated which artifacts are present in the output model and what their sources are.

The input model that is used for each step of the validation is by Xia, Walter, Hery, et al. (2023) with fiber\_0 which is viewed from the angle  $\theta_i = 0$ , so orthogonally to the fiber.

One element that will be visible in each test is a colorful noise pattern. This is due to the sample amount that was used for rendering, which is 1 million samples for the whole model. That results in 25 samples per pixel for the used dimension of  $200 \times 200$  pixels.

## 4.1 Single fiber

The main validation method for the framework is to compare the output for a single fiber to the model that was used as an input for the multi fiber model. If everything is implemented correctly the output model should be the same as the input model aside from possible small differences due to the Monte Carlo Integration.

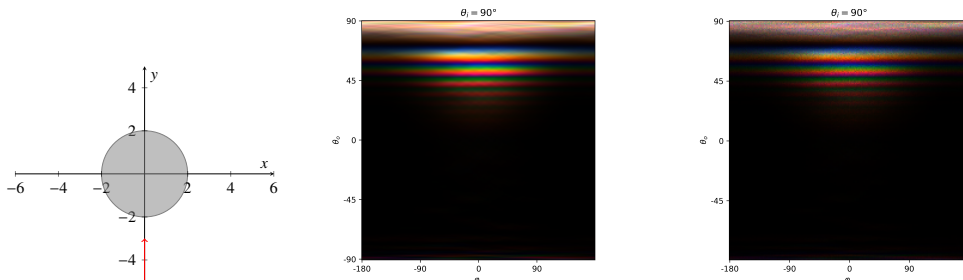


Figure 4.1: Comparison of the input model (middle) and the output model (right) for a single fiber. The left image shows the position of the fiber, as well as the initial direction.

From the comparison in figure 4.1 it can be seen that the details of the output model are very similar, aside from the lobe that is mostly missing at the grazing angles around  $90^\circ$ .

In 4.2 it can also be seen that a grid-like structure as an input results in the same structure in the

## 4.2. TWO FIBERS

---

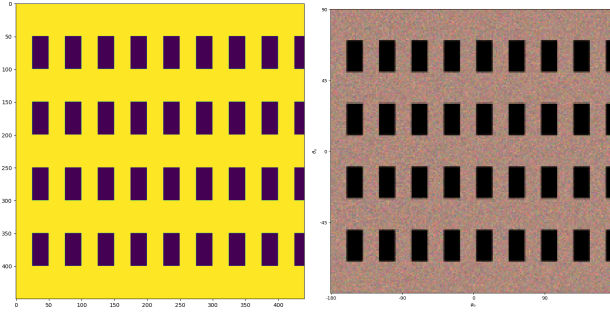


Figure 4.2: The output of the single fiber arrangement, when the input is set as a grid structure, where every wavelengths is the same.

output. This means that there are no warping artifacts in the model for single fibers and thus also for multiple fibers.

## 4.2 Two fibers

Another validation method is to compare the output for two fibers close together. The approximate shape of the output can be reasoned about intuitively. This way it is possible to examine if the outputting model has a similar shape.

In the example of the two fibers the fibers are assumed to be circular cylinders with the model being the same for every longitudinal angle  $\varphi_i$ . With this assumption, all the rays that just hit one fiber and then leave the boundary of the bundle should simply be the input model for the combination of input and output direction.

In this case, the expected output would be the input model, but with a dark line going down the  $\theta_o$ -s, since that is where the output has to have the least radiance. This is because the ray will need to pass through at least two fibers to reach this direction, instead of the other directions, which can be reached using just one bounce.

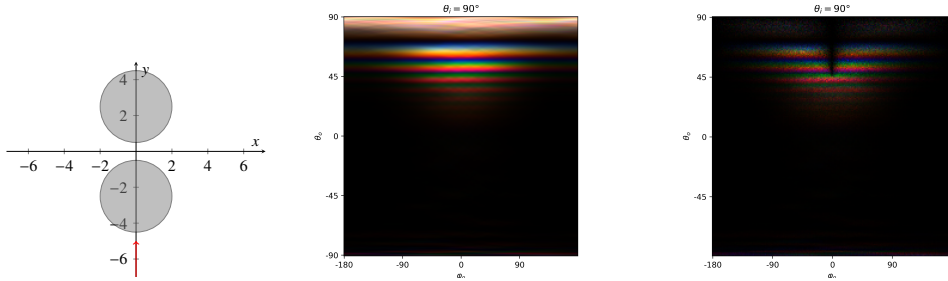


Figure 4.3: Comparison of the input model (middle) and the output model (right) for two fibers that are side-by-side. The left image shows the position of the fibers, as well as the initial direction.

As it can be seen in figure 4.3 there is indeed a darker column in the forward direction. So the

## CHAPTER 4. VALIDATION

---

output does line up with what was expected from the arrangement. Thus the change of magnitude for more than one interaction works correctly in the framework. Since the framework calculates one bounce at a time and doesn't change any behaviour depending on the depth of a bound aside from stopping at a maximum depth, it can be assumed that it works correctly for any number of bounces as long as the accuracy of floating point numbers is not exceeded.

## 4.2. TWO FIBERS

---

# 5

# Results

---

In the following, the outputs of the framework, as well as the resulting effects are examined. The chosen arrangements are circular cylinders with different densities and sizes, as well as an elliptical arrangement.

As a reference for the results the used input model can be seen in 5.1. At grazing incident angles this model displays a more uniform lobe in the forward direction with faint lines passing through it. The lines might stem from the rough surface that this model is based on.

As the incident angle moves towards  $\theta_i = 0^\circ$  lines along  $\varphi_o$  emerge. Especially in these lines, the difference in diffraction angle for the different wavelengths can be seen due to their chromatic aberration.

All of the results were created using 25 samples of the wavelength spectrum from 400 nm to 700 nm. Each rendering had a total of 1 million samples and the output model has the dimensions of  $200 \times 200$  pixels, which corresponds to 25 samples per pixel.

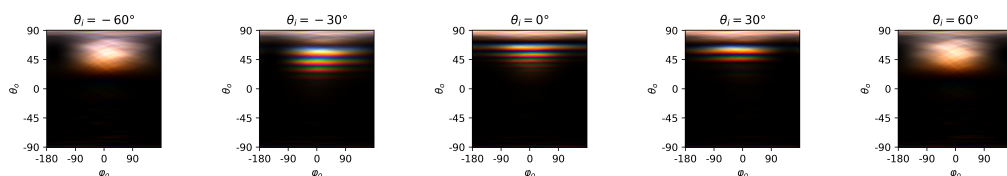


Figure 5.1: The input model for a single fiber, where all the wavelengths are overlapped to show the differences in the scattering.

## 5.1. CIRCULAR ARRANGEMENT

---

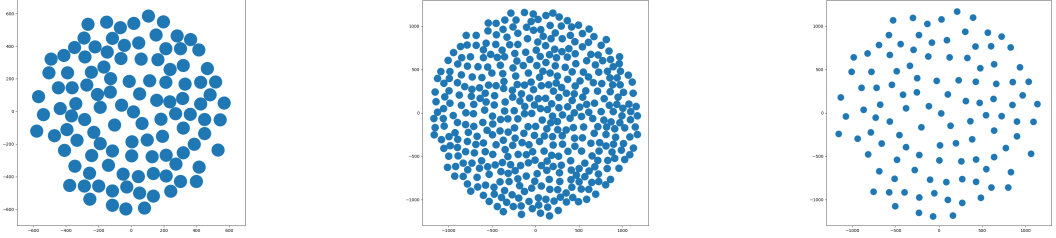


Figure 5.2: The arrangements of the three examined circular bundles. The one on the left shows the low radius structure. The one in the middle is the one with the doubled radius and the one on the right is the doubled radius with a lower density.

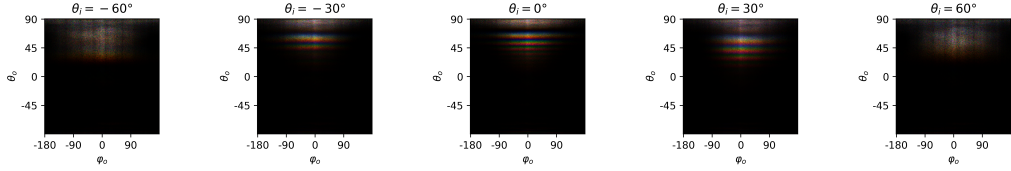


Figure 5.3: The output model for a circular arrangement of fibers with a radius of  $600\mu\text{m}$ , which is tightly packed.

## 5.1 Circular arrangement

The first bundle of fibers that is examined is a circular arrangement, that is generated using Poisson Disk Sampling. The circular shape is created by rejecting all samples that are outside of a bounding circle with a given radius.

In 5.3 the resulting model for a low density bundle is shown. The structure of the input model is preserved, which can especially be seen in the  $\theta_i = 90^\circ$  direction, where the scattering comes in the form of lines along the  $\varphi_o$  direction. These structures appear more blurry in the output model since the tracing over the fibers blurs all the effects uniformly with each bounce. This is due to the uniform shifting inside the fibers during each step.

The output model also preserves differences in diffraction angles for the different wavelengths, which comes from the fact that the light of different wavelengths is handled separately from one another. Thus the blur happens separately in each wavelength.

For the model in 5.4, the radius of the bundle was doubled. Interestingly there is no considerable difference between this model and the one of 5.3. The only major difference that can be found by comparing the two models side-by-side is that the scattering at the grazing angles appears more uniform since it has been scattered more often. This uniformity is also slightly reflected in the

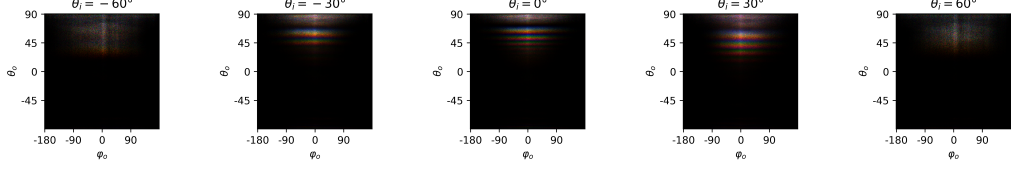


Figure 5.4: The output model for a circular arrangement of fibers with a radius of  $1200\mu\text{m}$ , which is tightly packed.

other angles, but it is most obvious in the grazing angles.

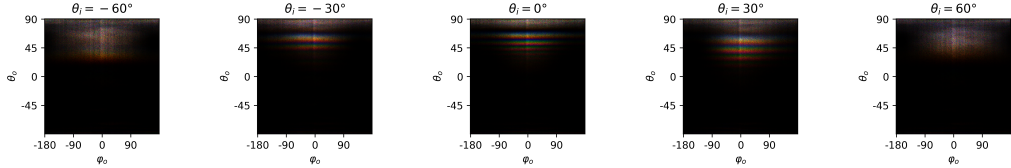


Figure 5.5: The output model for a circular arrangement of fibers with a radius of  $1200\mu\text{m}$  and a lower density of fibers.

The last circular arrangement that is investigated is a low density structure. 5.5 shows the output model for an arrangement that follows the third structure from 5.2. Compared to the high density arrangement with the same radius in 5.4 all elements of the input model are spread out along  $\varphi_o$ . This results from the higher chance for rays to pass through the bundle after only a few bounces. Thus they carry more radiance in all outgoing directions.

## 5.2 Elliptical Arrangement

In 5.7 the output model for an elliptical arrangement (5.6) can be seen. The arrangement is generated similarly to the circular one using Poisson Disk Sampling, but in this case, the bounding shape for discarding the outliers is an ellipse instead of a circle.

In this case, the interesting changes appear when  $\varphi_i$  changes, since the structure is not circular anymore and thus from different positions on the surface of the structure, different surroundings exist. At  $\varphi_i = 0^\circ$  the incident rays are pointed at the wide side of the ellipse, which means that

### 5.3. RENDERED

---

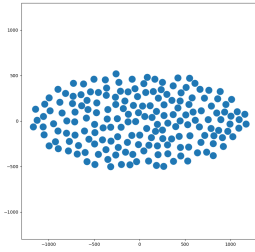


Figure 5.6: The arrangement of the fibers in the elliptical structure.

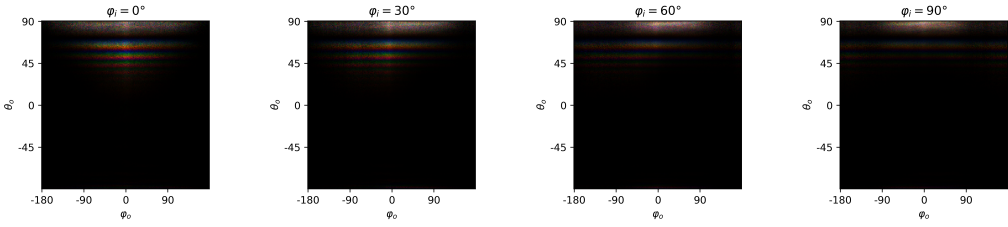


Figure 5.7: The results for an elliptical fiber structure. From left to right the input direction changes from  $\varphi_i = 0^\circ$  to  $\varphi_i = 90^\circ$ .

the shorter paths through the bundle are forwards facing, while the side facing ones are the ones that require more bounces on average. That causes similar lobes to appear as in the circular arrangements.

As  $\varphi_i$  increases the incident wavefront moves from the wide side of the ellipse towards the narrow one. In the output model, this is reflected by the spread of the elements evening out across the whole  $\varphi_o$  range, since the average amount of required bounces changes to be lower for the sides than the forward direction.

Thus the elliptical model shows that the shape of the structure plays a big role in how the output model changes the general shape of the input model.

## 5.3 Rendered

In this section, the output of the implementation in Mitsuba 3 (Jakob et al., 2022) is shown.

Each wavelength is calculated separately and converted into the representative CIE tristimulus values. These are then multiplied by the D65 illuminant factor for each specific wavelength and converted into RGB afterwards. Using that an RGB intensity image is generated for each wavelength and subsequently combined additively.

## CHAPTER 5. RESULTS

---

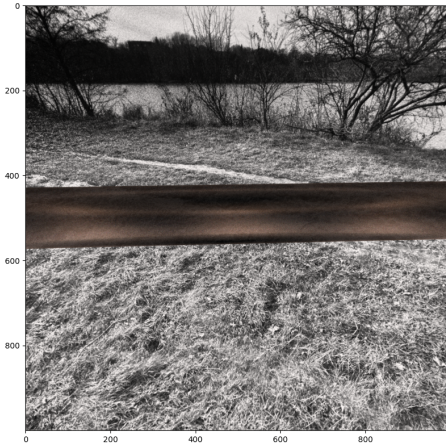


Figure 5.8: A rendered output of a single cylinder representing the bundle of fibers, rendered with separate wavelengths. Around the length of the cylinder  $\varphi_i$  is changed to simulate winding of the bundle.

The environment map was converted to grayscale for there to be no problem when calculating the wavelength intensities. By setting each environment to be the same greyscale image any outside source of colored lighting is diminished and any color in the rendered result can only come from the diffraction.

The result of the rays that pass through can also be seen by the transparency of the cylinder. A winding effect is created by changing  $\varphi_i$  along the length of the cylinder. That way the effect of the model can be more closely seen along the lower side of the model.

### 5.3. RENDERED

---

# 6

# Summary

---

In this thesis, a framework was developed to compute the light scattering of a bundle of fibers for different wavelengths. The framework was built by first aggregating the fiber bundle into a representation for the Mitsuba 3 renderer by Jakob et al. (2022) using parallel cylinders. Using this representation the light scattering was computed by tracing rays through the structure at different incident angles and by recording the outgoing radiance. The resulting data was then used to create a tabulated light scattering model, which was integrated into Mitsuba 3 to allow the rendering using an integrator, which allows for the outgoing position of a ray to be different from the initial position.

While investigating the light scattering of the fiber bundle, it was observed, that the light scattering shows a lot of the highlights of the input data, albeit blurred for the structure that was chosen in this thesis. It was also seen that the amount of blurring depends on the density, as well as the structure, of the bundle.

## 6.1 Future work

In the following, there are a few regions where the framework can be improved or further extended. The first two (6.1.1, 6.1.2) serve to improve the realism of the scattering model, while the latter two (6.1.3, 6.1.4) mainly serve to improve the computation time of the framework by reducing the dimensions of the input and output models.

### 6.1.1 Flyaway fibers

The flyaway fibers are the randomly spread out and oriented fibers which are not part of the main plies and which are singular. Their impact on the appearance of the material is not to be underestimated, as it can be seen in the work by Zhao et al. (2016). They are responsible for the fuzzy nature of many fabrics and textiles. Without wave-based approaches, their visual potential can't fully be reached, since many colourful glints and highlights are created by the wave model, as it can be seen in the work by Xia, Walter, Hery, et al. (2023) where the wave effects of singular models are shown.

## 6.1. FUTURE WORK

---

Including this addition to the novel yarn model would further improve the visual quality of the material. The structure of the flyaway fibers can be modelled using the parametric approach by Zhao et al. (2016) where they are modelled as different structures of fibers, which either loop back into the structure or point outside. Their distribution is fitted to the real models they analyzed.

The fiber light model can then be taken from the work by Xia, Walter, Hery, et al. (2023) where they present a model for the light transport of singular fibers with microstructures. This model introduces a lot of realistic colorful glints and highlights.

It could also be interesting to investigate the impact of the flyaway fibers on the far-field scattering of a ply or a whole yarn in cases where the single fibers cannot be seen anymore. This should add some additional sheen to the model, which might differ in its appearance from a sheen that simply depends on the angle equally over every wavelength.

### 6.1.2 Comparison against physical wave simulations

One effect that could not be captured by the approach of this thesis is the wave interaction that can occur between the fibers in the bundle. Modelling this effect would require physical wave simulations, which are comparatively expensive to compute. Which is why it was not possible in the scope of this thesis.

Inside the fiber bundles, a lot of additional wave interference might occur, due to the close proximity of the fibers. This leads to a high density of waves with the same wavelength, but different phases.

Similarly to how the wave interference for a singular fiber created a lot of colorful glints and softer highlights in the work by Xia, Walter, Michielssen, et al. (2020) this might result in even more highlights of this kind.

### 6.1.3 Optimized Input Model

The tabulated input model that was used in this thesis is 5-dimensional, because of which it takes up a lot of space and is relatively slow to query. Even with the approximations of a circular fiber, where the incident  $\varphi_i$  angle does not have to be taken into account and with a  $\theta_i$  resolution of 15 degrees, the model still takes up around 0.5 GB of disk space.

A major part of the calculation time in the framework is spent on querying of the tabulated data for the input model since it is a high dimensional table of data, which also takes up a lot of space. Thus reducing the calculation time for the input model would be beneficial to the overall performance of the framework.

Xia, Walter, Hery, et al. (2023) have presented a method to fit parameters and noise textures to their model, which greatly reduces the amount of data that has to be stored and accessed. To

achieve this they used two wavelet noise textures and fitted the amount of different frequency bands of the noise texture to the data. In this case, wavelet noise was used, because it is almost completely bandlimited, which makes it a good choice when different frequency bands are combined.

These noise textures are used to approximate the noisy speckle patterns on the inside of the model, while the shape of the scattering lobe is approximated using an analytic model. The analytic model that is used by Xia, Walter, Hery, et al. (2023) is a combination of the diffraction term by Benamira and Pattanaik (2021), as well as the reflection term by d'Eon et al. (2011). This results in two noise textures that are 3-dimensional each, which reduces the required disk space to around 10 MB according to Xia, Walter, Hery, et al. (2023).

### 6.1.4 Optimized Output Model

Accessing the 5d tabulated model is a relatively expensive operation since it has to be accessed and interpolated for each intersection that happens with the geometry that uses it. Thus it would be beneficial to optimize this process in some way so that the model can be accessed more efficiently. There are a few methods that could be useful.

One that is worth investigating is to train a neural network on the tabulated data and then to query the network instead of the 5d model. This would greatly reduce the amount of data that has to be stored and accessed since the neural network would only have to store the parameters of the model and not the whole model itself. The time required to query the data could also be reduced, depending on the architecture of the network.

Another approach that would require a bit more prior work would be to find a practical model with parameters that can be fitted to the data to closely resemble it. Depending on the structure of the model that is used, the fitting process could be realized using a simple least squares method, similar to the fitting in Xia, Walter, Hery, et al. (2023), or using a gradient descent method if the model parameters are differentiable.

For circular structures, like the one that was used as an example in this thesis, it could be beneficial to investigate how close the model can be approximated by just fitting a blur kernel to the input model. An effect hinting at this could be seen in 5, where the output model had similar highlights to the input, albeit blurred.

This optimization could not be done during the thesis, since it would have gone outside the time scope of the work.

## 6.1. FUTURE WORK

---

# Bibliography

---

- Aliaga, C., C. Castillo, D. Gutierrez, M. A. Otaduy, J. Lopez-Moreno, and A. Jarabo (2017). “An appearance model for textile fibers”. In: *Computer Graphics Forum*. Vol. 36. 4. Wiley Online Library, pp. 35–45.
- Benamira, A. and S. Pattanaik (2021). “A combined scattering and diffraction model for elliptical hair rendering”. In: *Computer Graphics Forum* 40.4, pp. 163–175. eprint: <https://onlinelibrary.wiley.com/doi/pdf/10.1111/cgf.14349>. URL: <https://onlinelibrary.wiley.com/doi/abs/10.1111/cgf.14349>.
- d’Eon, E., G. Francois, M. Hill, J. Letteri, and J.-M. Aubry (2011). “An energy-conserving hair reflectance model”. In: *Computer Graphics Forum*. Vol. 30. 4. Wiley Online Library, pp. 1181–1187.
- Irawan, P. and S. Marschner (2012). “Specular reflection from woven cloth”. In: *ACM Transactions on Graphics (TOG)* 31.1, pp. 1–20.
- Jakob, W., S. Speierer, N. Roussel, M. Nimier-David, D. Vicini, T. Zeltner, B. Nicolet, M. Crespo, V. Leroy, and Z. Zhang (2022). *Mitsuba 3 renderer*. Version 3.0.1. <https://mitsuba-renderer.org>.
- Marschner, S. R., H. W. Jensen, M. Cammarano, S. Worley, and P. Hanrahan (2003). “Light scattering from human hair fibers”. In: *ACM Transactions on Graphics (TOG)* 22.3, pp. 780–791.
- Sadeghi, I., O. Bisker, J. De Deken, and H. W. Jensen (2013). “A practical microcylinder appearance model for cloth rendering”. In: *ACM Transactions on Graphics (TOG)* 32.2, pp. 1–12.
- Xia, M., B. Walter, C. Hery, O. Maury, E. Michielssen, and S. Marschner (2023). “A Practical Wave Optics Reflection Model for Hair and Fur”. In: *ACM Transactions on Graphics (TOG)* 42.4.
- Xia, M., B. Walter, E. Michielssen, D. Bindel, and S. Marschner (2020). “A wave optics based fiber scattering model”. In: *ACM Transactions on Graphics (TOG)* 39.6, pp. 1–16.

## BIBLIOGRAPHY

---

- Xu, Y.-Q., Y. Chen, S. Lin, H. Zhong, E. Wu, B. Guo, and H.-Y. Shum (2001). “Photorealistic rendering of knitwear using the lumislice”. In: *Proceedings of the 28th annual conference on Computer graphics and interactive techniques*, pp. 391–398.
- Zhao, S., F. Luan, and K. Bala (2016). “Fitting procedural yarn models for realistic cloth rendering”. In: *ACM Transactions on Graphics (TOG)* 35.4, pp. 1–11.